HIGH-EFFICIENCY ION MOBILITY COUPLED MALDI MS FOR TISSUE IMAGING OF ENDOGENOUS COMPOUNDS

Waters
THE SCIENCE OF WHAT'S POSSIBLE.™

[1]Emmanuelle Claude, [2]Paul J Trim, [1]Marten F Snel, [2]Malcolm Clench, [1]Thérèse McKenna,[1]Keith Compson, and [1]James I Langridge
[1] Waters Corporation, Manchester, UK; [2] Sheffield Hallam University, Sheffield, UK

INTRODUCTION

The two main instrumental challenges for the mass spectrometric analysis of tissue samples are sensitivity and specificity, *i.e.* how well the compound of interest can be distinguished from background ions. With the MALDI SYNAPT HDMS system, it is possible to improve the specificity of the analysis by reducing the precursor ion selection window to 1 Da in an MS/MS experiment and by the separation of ions by ion mobility prior to mass analysis. Ion mobility separation (IMS), separates ions according to their size, shape and charge state. Using this technique it is possible to separate different compound classes, giving additional confidence that the true distribution of an ion of interest is observed.

Here we use high efficiency ion mobility separations based on travelling wave (T-wave) technology[1] incorporated into the mass spectrometer. TriWave consists of three T-wave devices (see Figure 1). The first T-wave (Trap) is used to trap ions during the period when an IMS separation is being performed in the second T-Wave, thus greatly enhancing the efficiency of the IMS process. The final T-wave (Transfer) transports the separated ions to the TOF analyser. In addition fragmentation experiments can be performed in either or both the Trap and Transfer T-Wave regions *e.g.* providing Transfer fragmentation of two isobaric species that have been separated by their ion mobilities.

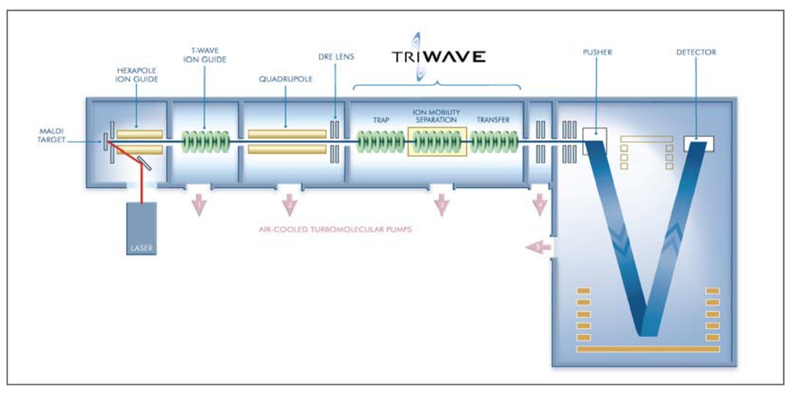

Figure 1. Schematic of the MALDI Synapt HDMS system, showing the TriWave Ion Mobility Separation device.

METHODS

The sample under investigation was a thin section of rat kidney. A 12 µm section was produced using a cryotome and deposited on thick aluminium foil. α-cyano-4-hydroxycinnamic acid (CHCA) matrix was applied evenly to the sample in several coats using an airbrush and the foil was mounted on a target plate.

The area to be imaged was selected using MALDI Imaging Pattern Creator (Waters Corporation, Manchester, UK) (see Figure 2). Data were acquired on a MALDI Synapt HDMS system (Waters Corporation, Manchester, UK) operated in HDMS mode over the m/z range of 10 to 1000.

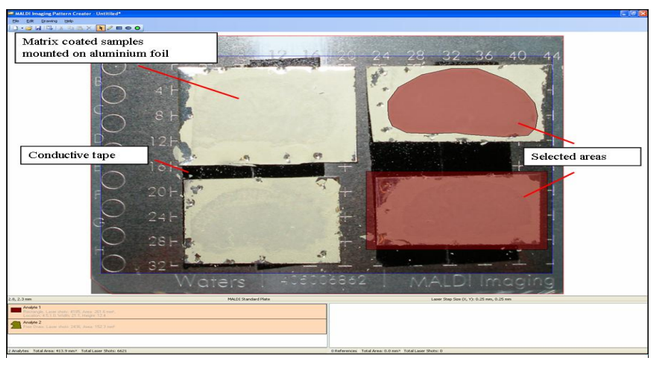

Figure 2. MALDI Imaging Pattern Creator is used to select the area(s) to be automatically imaged using MALDI SYNAPT HDMS.

Spatial resolution of 250 µm was selected and 600 laser shots were acquired per pixel at a laser repetition rate of 200 Hz. After acquisition HDMS data evaluation was performed using Driftscope (Waters Corporation, Manchester, UK). Data were converted into Analyze file format using MALDI Imaging Converter (Waters Corporation, Manchester, UK) for image analysis using BioMap (Novartis, Basel, CH) (see Figure 3).

RESULTS

Distribution of Phosphatidylcholines: Advantage of Exact mass and 1 Da precursor selection

Lipids play an important role in many biological processes, including the formation of cell membranes. Lipid families consist of highly similar structures, with difference in the aliphatic tails. This results in structures with similar m/z values(Figure 3).

Lipids with 2 Da mass difference usually have the same hydrophilic head group and differ by the number of double bonds in the fatty acid chains. In this example, the phosphatidylcholines (PC) of interest have m/z of 756.5524, 758.5696 and 760.5848.

It was possible to select the individual phospholipids, despite the complexity of the tissue sample, by using a 1 Da precursor ion selection window on the quadrupole and confirm their identities by MS/MS analysis. As illustrated in Figure 4, precursor ion 760.5848 was identified as MH^+ of PC (18:**1**, 16:0) and 758.5696 MH^+ of PC (18:**2**, 16:0). It was expected that the precursor ion 756.5524 would be MH^+ PC (18:**3**, 16:0) but the absence of the diagnostic fragment ions suggests otherwise.

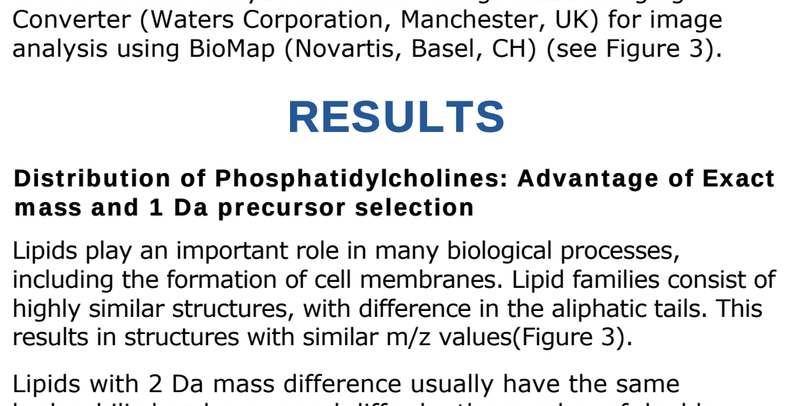

Figure 3. TOF mass spectrum obtained directly from kidney section.

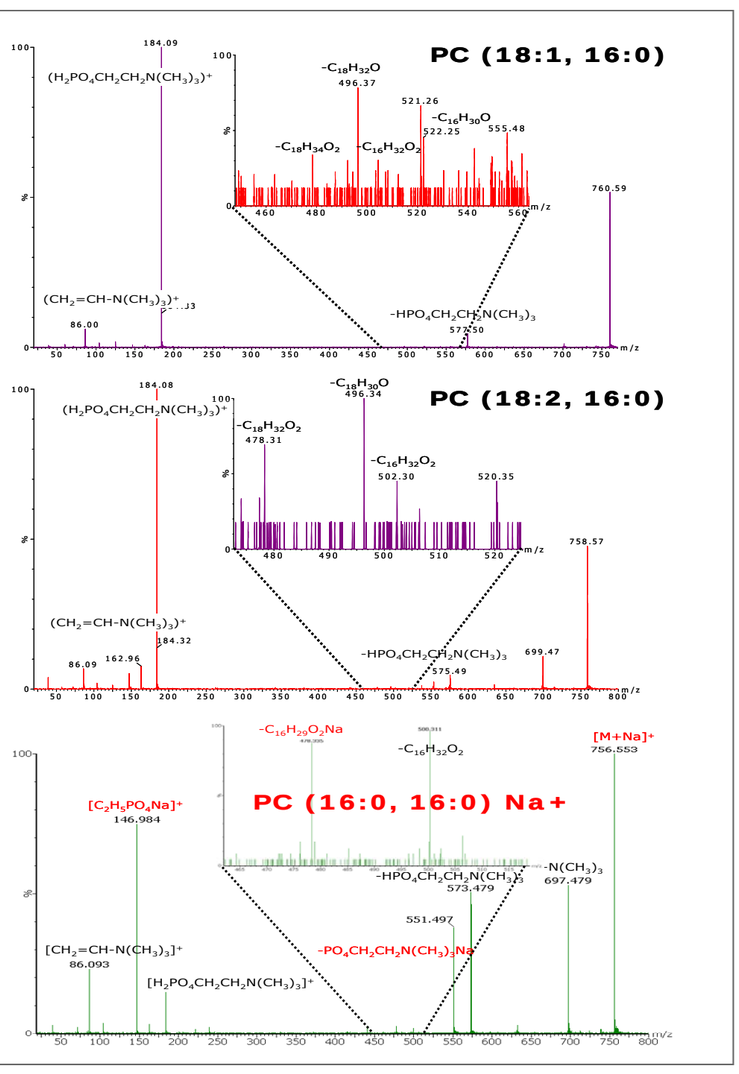

Figure 4. MS/MS spectra of m/z 756.5524, 758.5696 and 760.5848. The inset shows an enlargement of the m/z region 450–550 containing diagnostic fragment ions of the neutral loss of the fatty acid chain.

In this example, the mass accuracy of the neutral loss of the fatty acid chain fragments (m/z 478.335 and 500.311) for the precursor 756.5524 suggests it is the sodiated PC (16:0, 16:0) (Figure 5). Furthermore the hydrophilic head group fragment ions m/z 146.984 and 551.497 confirm the sodiated nature of the lipid.

Using the spatial information contained within the tissue imaging data set, ion intensity maps could be produced for the three phosphatidylcholines identified. The three images generated are shown in Figure 6. It can clearly be seen that the phospholipids localise differently, indicating that they have different biological functions.

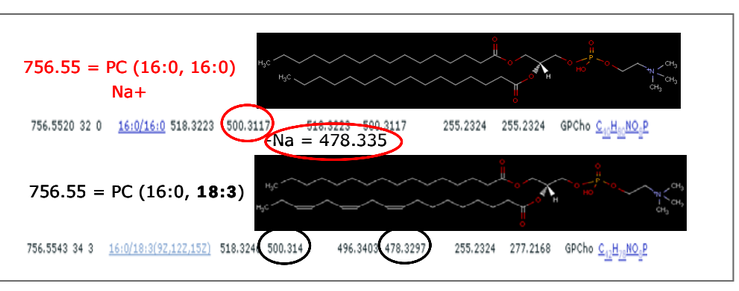

Figure 5. Theoretical interpretation of PC m/z 756.55, with fatty acid chain loss mass fragments.

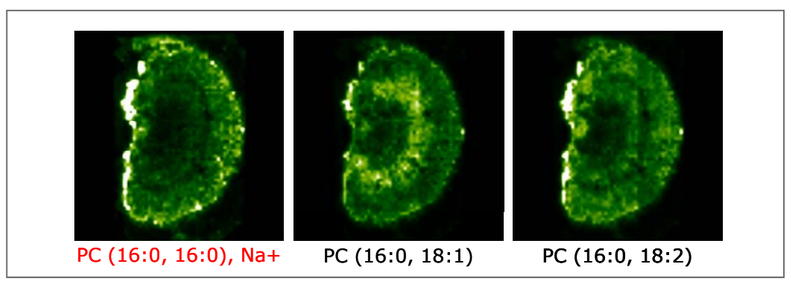

Figure 6. Ion intensity maps for the $[m+H]^+$ ions of PC (16:0, 18:1), PC (16:0, 18:2) and the $[m+Na]^+$ ion of PC (16:0, 16:0).

MALDI IMS imaging

The mass spectral data obtained during imaging experiments are often very complex. This can often lead to the situation where two or more isobaric species are present as illustrated in Figure 7 where two peaks with a nominal mass of 402 Da partially overlap, the larger of the two peaks (402.079 Da) was identified as the ^{13}C isotope of the sodiated dimer of CHCA, the other species (402.019 Da) could not be identified. Ion intensity maps were generated for both ions which show different distribution. (Figure 8). The higher intensity signal from the 402.019 Da species was observed in the centre of the kidney, however a strong signal was also observed outside the tissue (Figure 8 (a)). The unexpected signal outside the tissue is attributable to interference from the larger peak at 402.079.

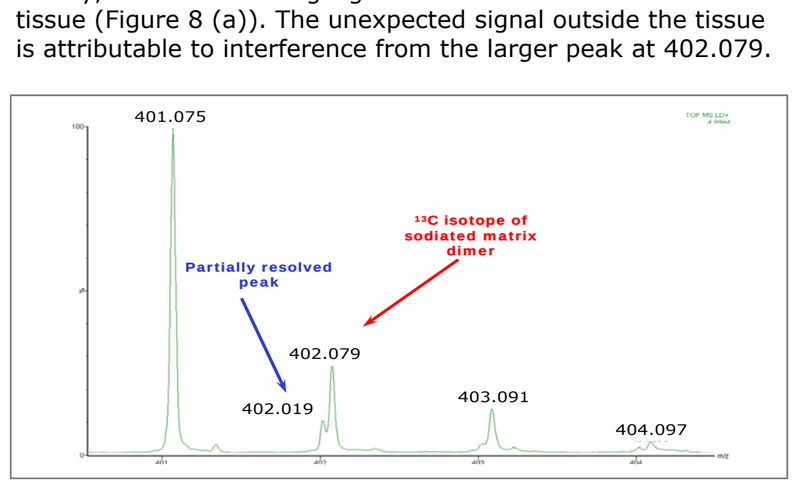

Figure 7. Partially overlapping peaks observed in an imaging experiment. This is a common occurrence owing to sample complexity.

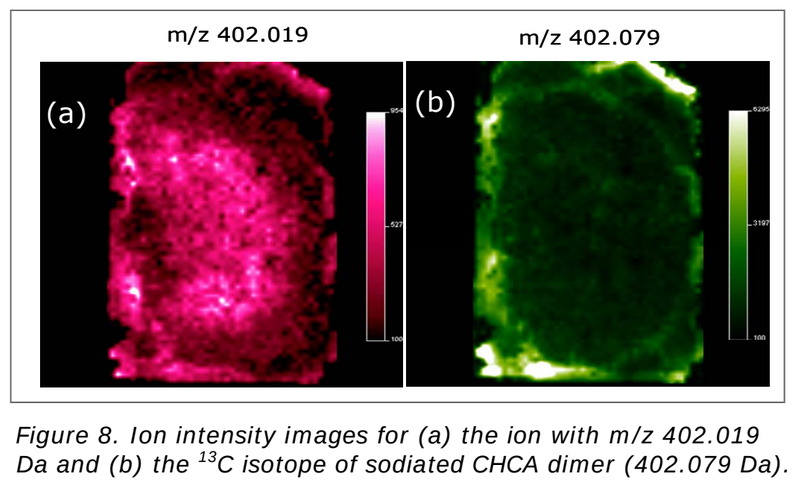

Figure 8. Ion intensity images for (a) the ion with m/z 402.019 Da and (b) the ^{13}C isotope of sodiated CHCA dimer (402.079 Da).

The use of IMS adds a further dimension of separation occurring post ionization, and as such lends itself to coupling with a MALDI imaging experiment,

The combined Driftscope mobility plot showing drift time (x-axis) *vs* m/z (y-axis) obtained from the kidney sample is shown in Figure 9. It can clearly be seen that ions of similar m/z i.e. those on the same horizontal line in the plot, are separated in the ion mobility dimension. The region around m/z 402 is enlarged and it can be observed that the ions discussed previously are separated in the ion mobility dimension. A full 3D data set consisting of m/z, IMS and intensity is acquired at every spatial position. This provides maximum flexibility for mining the data. It is also possible to perform a targeted experiment where only a small mobility and/or m/z range is acquired (not shown here).

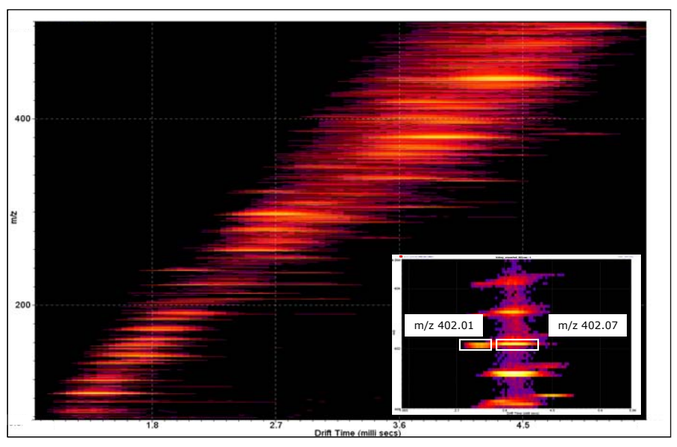

Figure 9. DriftScope data plot combined across the entire tissue section. Inset shows region (m/z 400.5–405 , IMS 2.3ms–5.0ms).

Exact mass drift time chromatograms of the 402.019 Da and 402.079 Da show the separation of the two species (Figure 10), when mass spectra are produced for the indicated drift times, 2.7 ms–3.3 ms and 3.4 ms–4.1 ms respectively, almost complete separation is achieved.

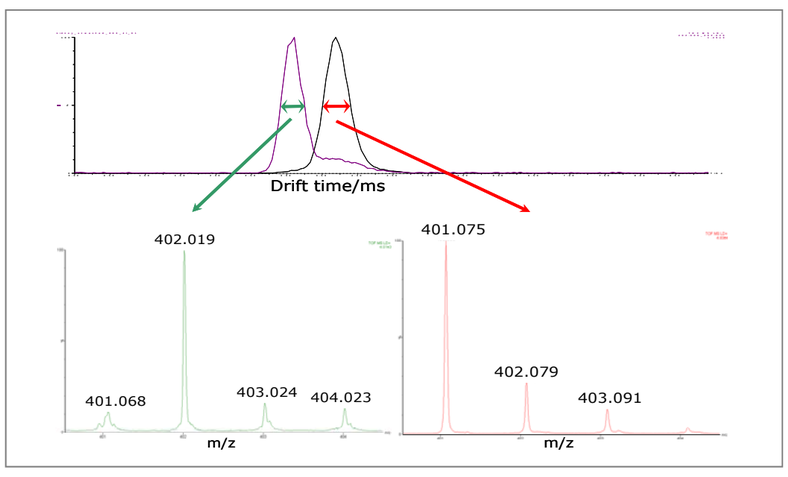

Figure 10. Separation of two isobaric ions based on their ion mobility. Top: Exact mass drift time chromatograms for m/z 402.019 and 402.079, bottom: mass spectra from selected IMS regions show effective separation.

When selected drift times are used for generating ion images of these isobaric components, distinctly different images are produced. After ion mobility separation, the ion intensity of the 402.019 Da ion, Figure 11(a), is localised in the centre of the tissue with very little intensity outside the tissue showing that it was possible to remove the interfering intensity contribution from the matrix ion (*c.f.* Figure 8(a)).

The intensity distribution of these ions observed with ion mobility is typical of distributions for endogenous species.

The image of the interfering matrix ion is similar with and without IMS separation, as the intensity contribution made by the 402.019 Da ion was very limited. This can be seen by comparing Figures 8(b) and 11(b).

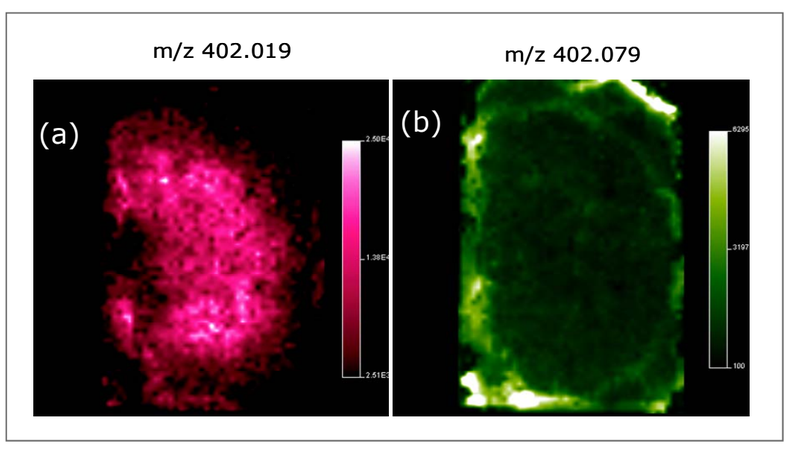

Figure 11. (a) Ion image of m/z 402.019 with IMS (2.7 ms–3.3 ms) and (b) image of m/z 402.079 (interfering background ion), with IMS (3.4 ms–4.1 ms).

CONCLUSION

- **Using MALDI orthogonal acceleration TOF mass spectrometry on a MALDI Synapt HDMS system, high resolution exact mass MS and MS/MS data were obtained directly from tissue.**
- **The phosphatidylcholines were characterised directly from tissue, using exact mass MS/MS data acquired with a precursor ion window of 1Da.**
- **The combination of high efficiency ion mobility separation with MALDI provides a unique separation dimension to further enhance mass spectrometric imaging.**
- **IMS can be used to produce images without interference from background ions of similar mass. This can remove ambiguity from imaging experiments and lead to more precise localisation of the compound of interest, e.g. drugs and metabolites.**
- **HDMS has the potential to reduce the complexity and improve confidence in imaging experiments.**

REFERENCES

1. K. Giles, S. Pringle, K. Worthington, D. Little, J. Wildgoose, R. B ateman, *Rapid Commun. Mass Spectrom.*, **2004**; 18: 2401-2414

50 YEAR LEGACY
VISION ■ CONTRIBUTION ■ ADVANCEMENT

TO DOWNLOAD A COPY OF THIS POSTER, VISIT WWW.WATERS.COM/POSTERS

720002767en